

Technical Report

Title: *Summary of Surrogate Core Analyses*

Document ID: TR-07-02


Authors: Richard Jackson and Sean Sterling

Revision: 1

Date: April 15, 2008

**DGR Site Characterization Document
Intera Engineering Project 06-219**



Intera Engineering DGR Site Characterization Document		
Title:	Summary of Surrogate Core Analyses	
Document ID:	TR-07-02	
Revision Number:	1	Date: April 15, 2008
Author(s):	Richard Jackson and Sean Sterling	
Technical Review:	Kenneth Raven, Ian Clark, Tom Al; Dylan Lohowy, Monique Hobbs (OPG)	
QA Review:	John Avis	
Approved by:	 Kenneth Raven	

Document Revision History		
Revision	Effective Date	Description of Changes
0	November 15, 2007	Initial Issue
1	April 15, 2008	Conversion from Technical Memorandum to Technical Report

TABLE OF CONTENTS

1	INTRODUCTION	1
2	BACKGROUND.....	1
3	METHODS OF CORE SAMPLING & PRESERVATION	1
	3.1 Drilling Program.....	1
	3.2 Core Recovery & Preservation	2
4	RESULTS	3
	4.1 Geochemistry	3
	4.2 Mineralogy & Petrography	5
	4.3 Petrophysical Measurements	9
	4.4 Diffusion Measurements.....	13
	4.5 Porewater Extraction	15
	4.5.1 UniBern.....	16
	4.5.2 University of Ottawa.....	19
5	DATA QUALITY AND USE	20
6	CONCLUSIONS	20
7	REFERENCES	20

LIST OF TABLES

Table 1	Core Testing Program.....	2
Table 2	Summary of Core Collected, Preservation Quality and Testing Laboratory	3
Table 3	Whole Rock Analysis by ICP-OES (Actlabs, 2006b)	4
Table 4	Trace Element Analysis by Fusion-ICP-OES (Actlabs, 2006b).....	4
Table 5	Detailed Petrography of OS1-074.80.....	5
Table 6	XRD Identification of Minerals Present in OS1-074.80.....	7
Table 7	Mineralogical analysis by the University of Bern (Waber et al., 2007)	8
Table 8	Petrophysical Parameters from OS1-071.98 by Terra Tek.....	9
Table 9	Petrophysical Parameters from OS1-069.32 (CoreLab, 2006).....	10
Table 10	Results from Mercury Injection Tests	11
Table 11	Porosity and Grain Density Measurements for Samples from OS1	13
Table 12	Summary of Diffusion Properties of Surrogate Cores by the Through-Diffusion Method.....	14
Table 13	Summary of Diffusion Properties for Surrogate Cores by X-Ray Radiography	15
Table 14	Apparent Concentrations of Chloride and Bromide Ions in Pore Water from OS1-56.49	17
Table 15	Composition of Extracted Pore-Water Aliquots and the Artificial Pore Water (APW)	17
Table 16	Crush and Leach Concentrations (Clark and Mohapatra, 2007).....	18

LIST OF FIGURES

Figure 1 OS1-074.80 Width = 2.3 mm Polarized Light (Actlabs, 2006a)..... 6
Figure 2 OS1-074.80 Width = 2.3 mm Reflected Light (Actlabs, 2006a)..... 6
Figure 3 Iron-Rich Cubes (possibly ankerite) Shown at x2200 by Scanning Electron Microscopy (Actlabs, 2006) 7
Figure 4 Energy Dispersive Spectra of Iron-Rich Cubes Shown in Figure 3 (Actlabs, 2006)..... 8
Figure 5 Pore Volume Determination by Boyle’s Law Method (Courtesy of CoreLab)..... 10
Figure 6 Pulse-decay Permeameter (Courtesy of CoreLab) 11
Figure 7 Gravimetric Water Content Obtained by Drying at 105°C as a Function of the Sum of Sheet Silicates, i.e., Clay Minerals (from Waber et al., 2007)..... 12
Figure 8 Specific Surface Area Versus Percentage of Clay Minerals (from Waber et al., 2007)..... 12
Figure 9 Saturated Core Samples from Borehole OS1, St. Mary’s Cement Quarry, Bowmanville 13
Figure 10 Determination of D_e and α for Clay-rich Core from St. Mary’s Quarry..... 14
Figure 11 Diffusion Profile by X-ray Radiography on Sample OS1-044, Parallel to Bedding..... 15
Figure 12 Anion Concentrations in Aqueous Extract Solutions of Cobourg Limestone Samples as a Function of Solid:Liquid Ratios. 16
Figure 13 Cation Concentrations in Aqueous Extract Solutions of Cobourg Limestone Samples as a function of Solid:Liquid Ratios. 17
Figure 14 Stable Isotopes of Oxygen and Hydrogen for the Bowmanville Cores..... 19

LIST OF APPENDICES

APPENDIX A Photograph of the Cobourg Formation at St. Mary’s Quarry
APPENDIX B Photographs of Cores
APPENDIX C Diffusion Properties for Surrogate Cores by X-ray Radiography

1 Introduction

This Technical Report (TR) summarizes the results obtained from geochemical, mineralogical and petrophysical tests on the surrogate cores that were conducted during 12 month period following core recovery in August 2006.

The results described in this Technical Report constitute one component of Intera Engineering Ltd. (2006a) Geoscientific Site Characterization Plan (GSCP) for the Bruce Deep Geologic Repository (DGR). A potential DGR site is being investigated for disposal of low and intermediate level radioactive waste at the Bruce site near Tiverton Ontario. The GSCP describes recommended methods and approaches to acquire the necessary geoscientific information to support (1) the development of descriptive geosphere models of the Bruce Nuclear site and (2) the preparation of an environmental assessment and site preparation and construction license application for submission to the Canadian Nuclear Safety Commission.

Work described in this Technical Report was completed in accordance with Intera Test Plan TP-06-01 – Off-site Core Collection and Preservation (Intera Engineering Ltd., 2006b), prepared following the general requirements of the DGR Project Quality Plan (Intera Engineering Ltd., 2007a).

2 Background

Several off-site initiation activities were identified in the GSCP as requiring completion prior to commencement of Phase I investigations of the proposed DGR location at the Bruce site. Requirement 1.3 of the GSCP – Refinement of Core Porewater Extraction and Simulation Methods - called for the collection of core from the argillaceous Ordovician formations of interest at locations off the Bruce site in a saline groundwater setting. This core – referred to as ‘surrogate core’ – is for use in a laboratory testing program to refine methods for petrophysical measurement and the extraction and analysis of rock core porewater from what are anticipated to be very low permeability formations at the DGR.

The formation of particular interest is the Cobourg argillaceous limestone, which is the host formation for the proposed Bruce DGR. The refined methods of laboratory porewater extraction and testing of rock core are being applied in the Phase 1 drilling and testing program undertaken as part of the Bruce DGR site characterization work. These methods will improve the quality of geoscientific data to be determined from intact rock cores at the Bruce site. By recovering Cobourg Formation cores from shallow depths at the St. Mary’s cement quarry near Bowmanville, Ontario for use in this testing program, these cores have provided surrogate materials for method development and testing prior to the recovery of Cobourg cores from the DGR1 and DGR2 boreholes and thus removed the need to use DGR cores to initiate such testing.

3 Methods of Core Sampling & Preservation

3.1 Drilling Program

The drilling location selected for the recovery of samples of Cobourg argillaceous limestone from a shallow saline groundwater environment was the St. Mary’s Cement Company quarry near Bowmanville, Ontario on the north shore of Lake Ontario. The drill-hole location was close to Lake Ontario and remote from hydraulic influences of the operating quarry and was labelled OS-1 (off-site borehole #1). Appendix A shows the exposed Cobourg formation in the St. Mary’s Cement quarry near the drilling location; the quarry was photographed by Dr. Derek Martin of OPG’s Geoscience Review Group during their visit to the site in 2006.

A continuous cored borehole was completed using rotary drilling methods to a depth of 77 m bgs. The drilling produced a core of 76 mm diameter, collected in 3 m length core runs. The drilling fluid was composed of Lake Ontario water that was labelled with approximately 1000 µg/L of sodium fluorescein (NaFI) to permit

quantification of potential drill-fluid contamination of the porewaters in the recovered cores.

3.2 Core Recovery & Preservation

Recovered core was digitally photographed in wooden core boxes and then logged before being preserved. Sample preservation included flushing with nitrogen, vacuum sealed and then vacuum sealing in aluminium foil-PE bags. Photographing and preserving of core were started within 15 minutes of core retrieval and were completed within 30 minutes of core retrieval from the borehole. Preserved cores were then weighed and labelled in accordance with the requirements of TP-06-01 (Intera Engineering Ltd., 2006b) identifying the length and midpoint depth of each core sample, date and time of core preservation, weight of labelled and preserved core, and intended laboratory. Recovered core that was not preserved is stored at the DGR core storage facility located at the Bruce Nuclear site in 3 m length core boxes at room temperature. Core photographs are presented in Appendix B.

Table 1 Core Testing Program

Project Manager & (Testing Laboratory)	Core Samples Received	Type of Testing
Dr. Martin Mazurek (<i>UniBern</i>) University of Bern Institute of Geological Sciences, Bern, Switzerland	OS1-031.03 OS1-051.49 OS1-052.76 OS1-056.49 OS1-062.43 OS1-076.90	Porewater extraction by out-diffusion, diffusive equilibration & advective displacement and characterization by Ni-en and aqueous extraction
Dr. Tom Al, (<i>UNB</i>) Department of Geology, University of New Brunswick, Fredericton, NB	OS1-044.57 OS1-075.97	Effective diffusion coefficients by through-diffusion cell and X-ray radiography
Dr. Ian Clark, (<i>UOttawa</i>) Department of Earth Sciences, University of Ottawa, Ottawa, ON	OS1-051.28 OS1-063.30 OS1-071.02	Porewater characterization for He and Ne gases and isotopes by crush & vacuum distillation, azeotropic distillation, stepped heating and diffusive equilibration
Dr. Mel Gascoyne, (<i>USGS</i>) Gascoyne GeoProjects, Pinawa, MN	OS1-050.09 OS1-054.35 OS1-067.87 OS1-068.28 OS1-073.86	Ultracentrifugation and major ions at USGS Lakewood CO by Z.E. Peterman and K. Scofield
Intera Engineering Ltd., (<i>CSF</i>) Core Storage Facility, Bruce Site, ON	OS1-033.73 OS1-059.34 OS1-062.66	Back-up cores for supplementary testing
Dr. Eric Hoffman, (<i>Actlabs</i>) Activation Laboratories, Ancaster ON	OS1-074.80	Geochemistry (oxides and elements), mineralogy (XRD and SEM) and petrography
Mr. Craig Whitney, (<i>CoreLab</i>) Core Laboratories, Houston TX	OS1-069.32	Porosity, permeability and high-pressure mercury injection
Mr. John Keller, (<i>TerraTek</i>) TerraTek, Salt Lake City UT	OS1-071.98	Porosity, fluid saturations and permeability

Table 1 lists the core testing program for each of the laboratories participating in Phase I of the GSCP and Table 2 lists the specifics of the individual preserved core samples and their destination. A total of 22 core samples

were preserved with a total of 4 m an average length of 18 cm. The longest preserved core samples (i.e., > 20 cm) were shipped to UniBern to allow them to test the advective porewater displacement method of porewater extraction. USGS results on ultracentrifugation are not reported in this TR.

Table 2 Summary of Core Collected, Preservation Quality and Testing Laboratory

Sample No.	Depth (m)	Bedrock Depth (m)	Core Length (cm)	Weight (g)	Seal Quality	Testing Laboratory (see Table 1)
OS1-031.03	31.03	11.7	24	> 2610	G	UniBern
OS1-033.73	33.73	14.4	20	2493.1	P	
OS1-044.57	44.57	25.2	19	2254.2	G	UNB
OS1-050.09	50.09	30.7	16	2037.5	G	USGS
OS1-051.28	51.28	31.9	20	2394.0	A	UOttawa
OS1-051.49	51.49	32.1	23	> 2610	VG	UniBern
OS1-052.76	52.76	33.4	29	> 2610	A	UniBern
OS1-054.35	54.35	35.0	23	> 2610	P	USGS
OS1-056.49	56.49	37.1	24	> 2610	G	UniBern
OS1-059.34	59.34	40.0	19	2360.0	P	
OS1-062.43	62.43	43.1	26	> 2610	G	UniBern
OS1-062.66	62.66	43.3	13	1581.2	VG	
OS1-063.30	63.30	44.0	22	> 2610	G	UOttawa
OS1-067.87	67.87	48.5	13	1480.6	G	USGS
OS1-068.28	68.28	48.9	19	2196.8	A	USGS
OS1-069.32	69.32	50.0	14	1690.2	G	CoreLab
OS1-071.02	71.02	51.7	16	1882.6	A	UOttawa
OS1-071.98	71.98	52.6	14	1703.1	A	TerraTek
OS1-073.86	73.86	54.5	16	1856.4	G	USGS
OS1-074.80	74.80	55.5	9	1153.2	G	Actlabs
OS1-075.97	75.97	56.6	11	1306.0	P	UNB
OS1-076.90	76.90	57.6	10	1151.6	G	UniBern

Seal Quality Legend: Very Good, Good, Average, Poor.

4 Results

4.1 Geochemistry

Core OS1-074.80 was analysed at Actlabs (2006b), Ancaster Ontario, for oxides and elemental geochemistry. Oxides are determined by a fusion technique in which the core sample is dissolved in a crucible in a muffle furnace at high temperature (~900°C) with a lithium metaborate-tetraborate flux. It is then analyzed by inductively coupled plasma mass spectrometry-optical emission spectrometry (ICP-OES) to yield a 'whole rock analysis'. These results are shown in Table 3.

Table 3 Whole Rock Analysis by ICP-OES (Actlabs, 2006b)

Oxide	Detection Limit (%)	Result (%)
SiO ₂	0.01	9.92
Al ₂ O ₃	0.01	2.7
Fe ₂ O ₃	0.01	1.22
MgO	0.01	1.67
MnO	0.001	0.025
CaO	0.01	45.75
TiO ₂	0.001	0.124
Na ₂ O	0.01	0.14
K ₂ O	0.01	0.69
P ₂ O ₅	0.01	0.06
Loss on Ignition	0.01	36.96
Total	--	99.26

Following the fusion step, the sample is analyzed for minor and trace elements by ICP-MS using argon plasma as the ionization source and a quadruple mass spectrometer to detect the ions produced. If sample concentrations exceed the upper detection limit, the sample is analyzed by ICP-OES, see Table 4. Organic carbon was analysed by infra-red spectroscopy and was estimated to be 0.1% [detection limit = 0.05%].

Table 4 Trace Element Analysis by Fusion-ICP-OES (Actlabs, 2006b)

Element	Detection Limit (ppm)	Results (ppm)	Element	Detection Limit (ppm)	Results (ppm)
Ag	0.5	<0.5	Tl	0.05	0.07
As	5	<5	V	5	21
Ba	3	59	W	0.5	2.1
Be	1	<1	Y	0.5	6.6
Bi	0.1	<0.1	Zn	30	<30
Co	1	<1	Zr	4	35
Cr	20	<20	La	0.05	9.15
Cs	0.1	1.5	Ce	0.05	18.9
Cu	10	10	Pr	0.01	2.01
Ga	1	3	Nd	0.05	7.54
Ge	0.5	<0.5	Sm	0.01	1.33
Hf	0.1	0.9	Eu	0.005	0.296
In	0.1	<0.1	Gd	0.01	1.18
Mo	2	4	Tb	0.01	0.2
Nb	0.2	2.3	Dy	0.01	1.12
Ni	20	<20	Ho	0.01	0.22
Pb	5	5	Er	0.01	0.62

Rb	1	25	Tm	0.005	0.09
Sb	0.2	<0.2	Yb	0.01	0.57
Sc	1	3	Lu	0.002	0.087
Sn	1	<1	U	0.01	1.18
Sr	2	444	Th	0.05	2.74
Ta	0.01	0.21	Li*	1	18

* Li was analysed by ICP following a total acid digestion.

4.2 Mineralogy & Petrography

Core OS1-074.80 was also analysed by x-ray diffraction (XRD) and thin-section petrography for mineralogy and by scanning electron microscopy for pore fabric. Thin-section petrography was conducted on behalf of Actlabs by Dr. Eva Schandl of Geoconsult, Toronto (Actlabs, 2006a). The sample consists predominantly of poorly sorted fossil fragments of various size, ranging from a few micrometers to 3 mm in diameter. The fragments are enclosed in a matrix of calcareous (partly re-crystallized) mud. Slumping and deformation of the fine-grained matrix is common, particularly around the larger fossil fragments, and dark veinlets (possibly Fe-stained) creating boudinage in some fossils. The fine-grained calcite matrix also contains inclusions of minute quartz grains, pyrite framboids, anhedral grains of pyrite, and marcasite aggregates. Halite was not identified in the rock. Table 5 summarizes the petrographic analysis.

Table 5 Detailed Petrography of OS1-074.80

Mineral	% Present	Grain size(mm)	Comments
Fossil Fragments	60	<0.1-3.0	A large variety of calcified fossil fragments make up a significant part of the rock. Several of the larger fragments are re-crystallized to fine-grained granular carbonates at the grain boundaries.
Carbonate	39	<0.1-1.0	The matrix consists of very fine-grained carbonate aggregates, some of which are Fe-stained. Carbonate also occurs in aggregates, forming up to 2-3 mm diameter domains, some of which re-crystallized to granoblastic aggregates
Quartz	0.5	50µm-0.2mm	Fine-grained, anhedral quartz and (less commonly) isotropic chalcedony is interstitial to the very fine-grained matrix carbonate. Quartz also occurs as inclusions in some of the re-crystallized fossil fragments.
Pyrite & Marcasite	0.5		Pyrite and marcasite were identified under reflected light. The pyrite occurs as minute framboids (single grains or aggregates) and as small, subhedral grains. Some pyrite aggregates partly replace the small fossil fragments. Anisotropic marcasite occurs in aggregates, some of which have cockscomb texture.

Figure 1 shows the calcareous fossil fragments in a fine-grain dark carbonate matrix and Figure 2 shows the pyrite framboids.

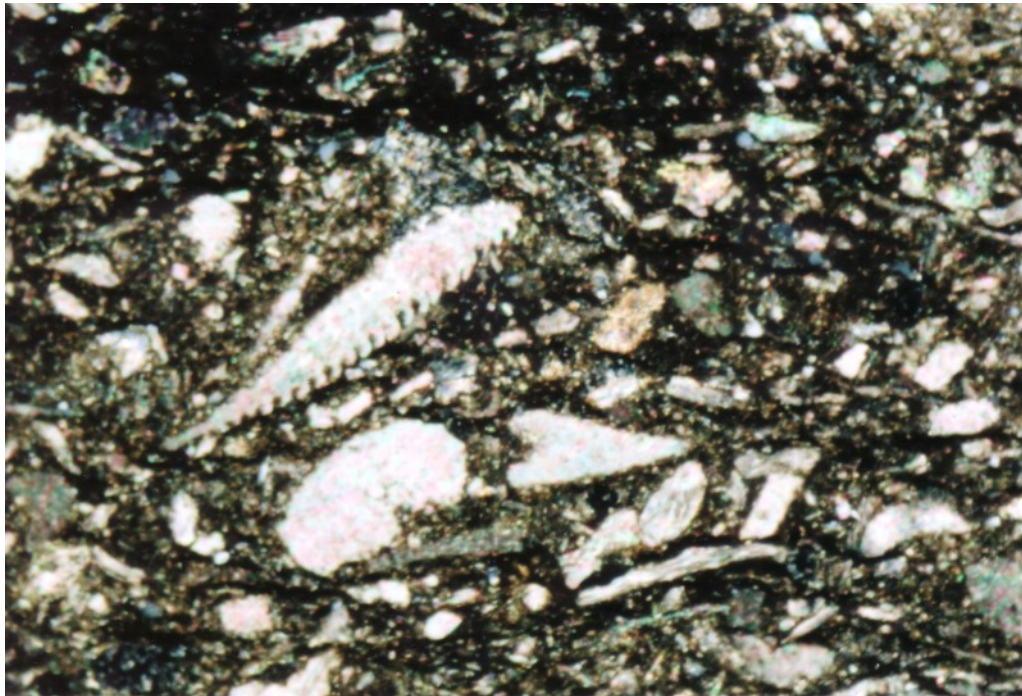


Figure 1 OS1-074.80 Width = 2.3 mm Polarized Light (Actlabs, 2006a)

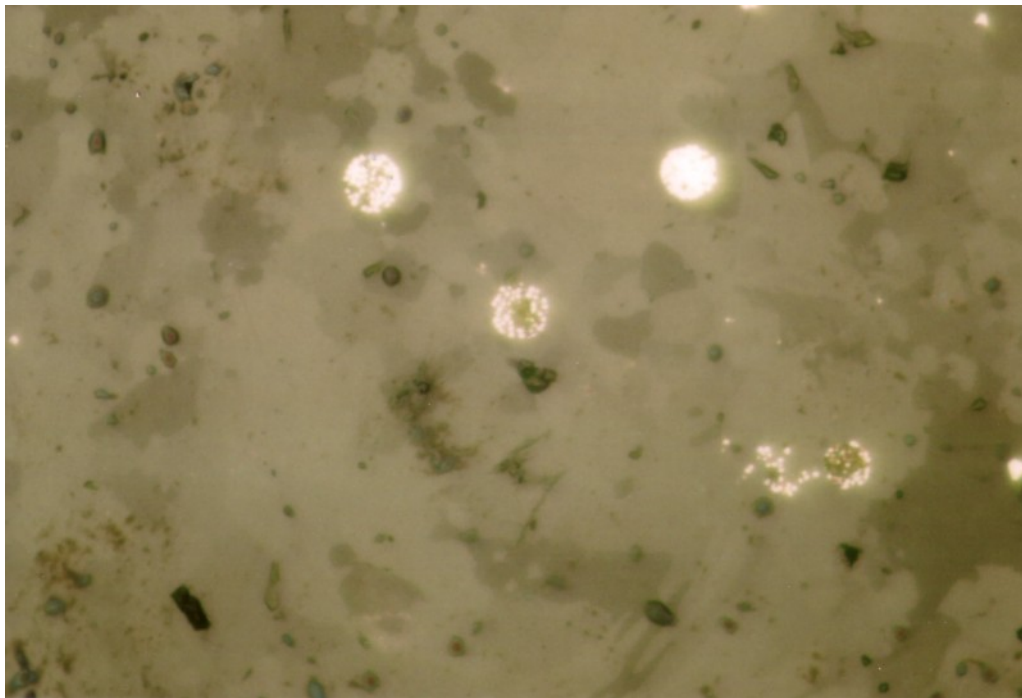


Figure 2 OS1-074.80 Width = 2.3 mm Reflected Light (Actlabs, 2006a)

Qualitative XRD analysis was conducted by Drs. K. Gabrielyan and A. Skowron of Actlabs. Both a whole rock analysis and clay mineral analysis were conducted. The results of the whole rock analysis are presented in Table 6. The sample is dominated by calcite with minor quartz and dolomite. The identification of the zeolite merlinoite in Table 6 was made by Actlabs, however, merlinoite typically occurs in volcanic rocks and pegmatites, thus there is considerable doubt about this identification.

Clay mineral identification was based on standard methods of glycolation and heating. Kaolinite was identified on the basis of the 0.7 nm peak that disappeared after heating at 550 °C. Illite was identified by the absence of any change to its 1 nm peak. Chlorite was identified by the increase in intensity of its 1.4 nm peak after heating to 550 °C. Magnesium calcite and quartz were dominant in the clay-size fraction.

Table 6 XRD Identification of Minerals Present in OS1-074.80

Identified Minerals	Approximate Concentration (%)
Calcite ($\text{Ca}_{0.97}\text{Mg}_{0.03}\text{CO}_3$)	87
Quartz	4
Merlinoite	6
Dolomite	3

Scanning Electron Microscopy coupled with elemental analysis by Energy Dispersive Spectroscopy (SEM/EDS) showed no measurable amount of halite (NaCl) present. The sample consisted of minerals composed of Ca, O and C with minor amounts of Si. Small iron-rich cubes were evident (see Figure 3) but EDS showed no evidence of sulphur. Rather, these cubes were shown to contain Ca, Fe, O and C (see Figure 4) and are likely to be ankerite, i.e., $\text{CaFe}(\text{CO}_3)_2$, which is possibly the unidentified mineral in Table 6 although its XRD pattern is almost identical to dolomite.



Figure 3 Iron-Rich Cubes (possibly ankerite) Shown at x2200 by Scanning Electron Microscopy (Actlabs, 2006)

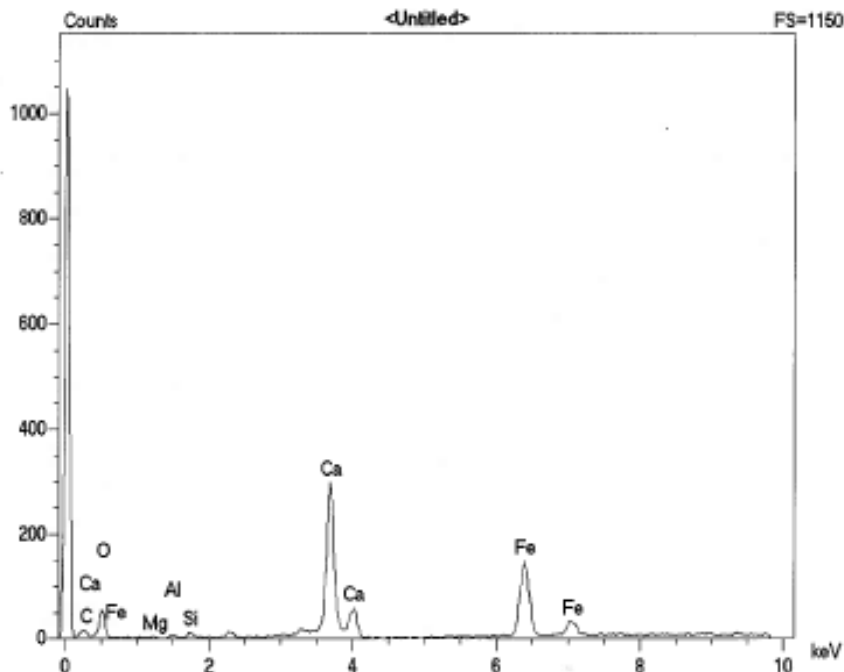


Figure 4 Energy Dispersive Spectra of Iron-Rich Cubes Shown in Figure 3 (Actlabs, 2006)

Mineralogical and geochemical analysis of four cores was also performed at the University of Bern in Switzerland. Their results are reported in Table 7. The petrological description of the core is based upon a quantitative analysis of sand, carbonate and clay fractions. Thus limestones are defined by the sand and clay concentrations, in which a 'sandy limestone' must exhibit a total of quartz + feldspar > 10% and a 'clayey' limestone must have > 10% of clay minerals. The designation of a 'limestone' is used when the total carbonate mineral concentration exceeds 25%; 'marl' is defined as a limestone with > 25% clay minerals. Thin sections were described as 'bioclastic, matrix-supported wackestone with relatively homogeneous petrographic characteristics.' The bioclasts were of the order of tens of micrometers to millimeters in size. No chloride or sulphate minerals were identified and no evidence of metamorphic or hydrothermal alteration noted. Iron sulphide minerals were found in similar concentrations in the cores examined at the University of Bern and by Actlabs (see Table 5).

Table 7 Mineralogical analysis by the University of Bern (Waber et al., 2007)

Sample No.		OS1- 51.49	OS1-52.76	OS1-56.49	OS1-76.90
Description	Units	clayey sandy limestone	sandy limestone-marl	clayey limestone	clayey limestone
Calcite	wt.%	63	56	70	80
Dolomite/Ankerite	wt.%	3	4	2	2
Quartz	wt.%	8	9	5	4
Albite	wt.%	<1	<1	<1	<1
K-Feldspar	wt.%	<1	2	<1	<1
Pyrite/ Marcasite	wt.%	0.6	0.4	0.6	1.5
Siderite	wt.%	2	2	2	1

Clay Minerals	wt.%	21	26	19	12
S	wt.%	0.3	0.2	0.3	0.8
C _{org}	wt.%	0.4	1.3	1.5	1.7
C _{inorg}	wt.%	8.2	7.5	8.9	9.9
Clay Minerals:					
Illite	wt.%	14	15	11	7
Illite /Smectite ML	wt.%	3	6	3	<1
Chlorite	wt.%	3	3	3	2
Kaolinite	wt.%	1	2	2	2

4.3 Petrophysical Measurements

Core OS1-071.98 was sent to Terra Tek in Salt Lake City for petrophysical analysis. The results are presented in Table 8. The gas saturation (S_g) of ~80% is estimated following the estimation of the pore volume ($PV=100\%$), water saturation (S_w) and oil saturation (S_o); it is computed as $S_g = 100 - S_w - S_o$. Thus, it contains errors acquired during each of these steps of measurement. Furthermore, because these measurements are conducted on un-stressed core that has undergone stress relaxation during coring, the pore volume has likely expanded by 5 – 10% from in-situ values (Jones and Owens, 1979). Thus, it is anticipated that the in-situ porosity is slightly lower than measured (i.e. closer to 2.0% compared to 2.2%) thus reducing the gas saturation.

Table 8 Petrophysical Parameters from OS1-071.98 by Terra Tek

Parameter	Result	Comment
Bulk density (g/cm ³)	2.69	On 'as-received' sample, i.e., containing pore fluids
Grain density (g/cm ³)	2.74	On 'as-received' sample
Dry grain density (g/cm ³)	2.75	
Porosity (% of bulk volume)	2.20	Boyle's Law method
Water saturation (% of pore volume)	16.2	Retort method
Mobile Oil saturation (% of pore volume)	4.0	Retort method
Gas saturation (% of pore volume)	79.7	Retort method
Gas-filled porosity (% of bulk volume)	1.76	
Bound hydrocarbon saturation (% of bulk volume)	0.16	
Bound clay water (% of bulk volume)	1.17	
Pressure-decay permeability (millidarcy, mD)	0.000041	$k = 4E-20 \text{ m}^2$

Core OS1-069.32 was sent to Core Laboratories (CoreLab) in Houston, Texas for mercury intrusion testing and other petrophysical tests. Two core plugs, with dimensions 2.3 cm x 2.5 cm (sample 1V) and 2.8 cm x 2.6 cm (sample 2H), were removed and tested. Sample 1V was sub-cored in the vertical direction, normal to the bedding planes, and measured while sample 2H was cored to estimate the horizontal properties of the core and measured. CoreLab first determined the pore volume of the core plugs by the Boyle's Law method with brine and oil in place (see Figure 5). The 'fresh-state' porosity is measured on the 'as received' core without prior fluid extraction; no residual porewater or oil is removed by this process. The total porosity, however, is measured on

the 'cleaned and dried' sample following fluid extraction by batch Soxhlet procedure and convection-oven drying.

Table 9 presents the 'as received' values that were obtained at a net confining pressure of 800 psi or 5.5 MPa applied hydrostatically. This net confining pressure simulates the effective stress on the core. Due to the apparent unsaturated state of the Cobourg Formation cores at St. Mary's quarry, i.e., pore pressure ~ zero, the effective stress ~ total stress. The horizontal stress is suspected of being 1.5 to 2.0 times higher than the vertical due to erosional unloading following deglaciation. Therefore, the net confining pressure of 800 psi may have been considerably larger than the core experienced in-situ at ~ 70 m depth.

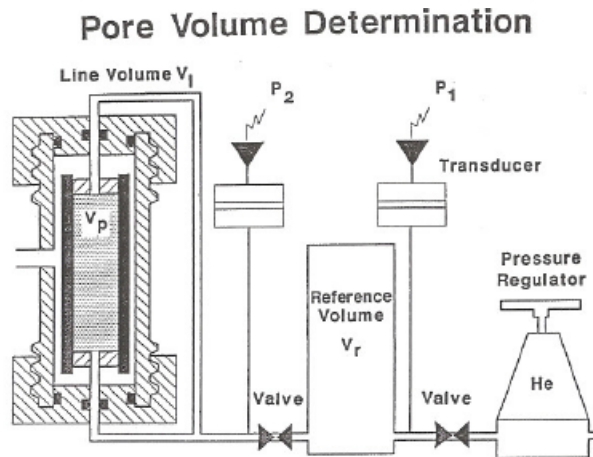


Figure 5 Pore Volume Determination by Boyle's Law Method (Courtesy of CoreLab)

Table 9 also shows the equivalent values after Soxhlet extraction and convection drying – i.e., 'cleaned & dried' state results – that remove the brine and oil contained in the core plugs. Grain density is calculated from bulk sample weight/grain volume. The porosity is calculated from the pore volume /bulk volume and the bulk volume = the sum of the pore and grain volumes. Both pore and grain volumes are determined using the Boyle's Law apparatus shown in Figure 5. These standard methods of petrophysics are described in TP-07-03 (Intera Engineering Ltd., 2007b).

Table 9 Petrophysical Parameters from OS1-069.32 (CoreLab, 2006)

Parameter	'As Received' State		'Cleaned & Dried' State	
	1V	2H	1V	2H
Weight (g)	31.097	36.525	30.730	35.699
Grain volume(cm ³)	11.658	13.749	11.347	13.194
Grain density (g/cm ³)	2.667	2.657	2.708	2.706
Porosity fraction	0.012	0.021	0.029	0.049
Pore volume (cm ³)	0.145	0.300	0.333	0.678
Pressure-decay permeability (mD)	0.0000224	0.0024204	0.0003	0.224*

* indicates that sample 2H fractured during testing

The porosity values indicate that the extraction of fluids from the two core plugs causes the pore volume of the plugs to more than double. This is due to the presence of brine and oil in the pore volume and suggests that the

combined saturations of oil and brine is > 50%, therefore the gas saturation, which comprises the balance of the pore volume is also ~ 50%. In comparison TerraTek measured a value of $S_g \sim 80\%$.

Both the porosity and the permeability results are higher in the horizontally-tested plugs than in the vertically-tested plugs – although sample 2H fractured during testing – indicating preferential gas flow in the horizontal plane. The permeability is measured by gas pulse, pressure decay at a net confining pressure of 1,000 psi (6.89 MPa). The permeameter is shown in Figure 6. Permeability is determined from the analysis of the decay of small pressure pulses (i.e., < 10 psi) transmitted through the core plug so that inertial flow resistance, gas slippage and gas compression are minimized (Jones, 1997). By working at a pressure of 1,000 psi, the measurement may be as much as 30% higher than the absolute permeability due to the very low permeability values reported (Craig Whitney, CoreLab, Houston, personal communication, August 2007). Nevertheless, the two samples have permeabilities in the nanodarcy range; the best estimate of the vertical permeability is $\sim 2E-20$ m², which is similar to that reported by TerraTek. The anisotropy in the permeability appears to be of the order of 100:1, i.e., horizontal > vertical from the ‘as received’ results.



Figure 6 Pulse-decay Permeameter (Courtesy of CoreLab)

Table 10 shows results from high pressure mercury intrusion tests to determine the entry pressure required to inject the non-wetting phase liquid mercury into the core plugs 1V and 2H. Full Hg saturation of the core plug is achieved at 55,000 psi (380 MPa), however the core plugs exhibit Hg penetration at ~ 3000 psi (21 MPa) and 1% Hg mercury saturation when the injection pressure reaches ~ 3500 psi (24 MPa). The mean pore-throat radius is of the order of 4 nm, which can be compared with a thickness of 0.2 nm of the electrical double layer of a colloid in 2M NaCl solution, i.e., 120 g NaCl/L, based upon the equation of Stumm (1992, p.49).

Table 10 Results from Mercury Injection Tests

Sample	Permeability (mD)	Porosity fraction	Approximate Threshold Pressure (psi)	Median Pore Throat Radius (µm)
1V	0.000006	0.011	3078	0.0043
2H	0.00002	0.029	2693	0.0035

The permeabilities presented in Table 10 are from the correlation developed by Swanson (1981); these are also in the nanodarcy range, but lower than the results presented in Table 8.

Studies conducted at the University of Bern (Waber et al., 2007) show that the water content of the rock – measured as a percentage by core-sample weight – is strongly dependent on the clay mineral content of the sample. Figure 7 shows this relationship for five samples of the St. Mary’s quarry core. Similarly, the specific surface area in square meters per gram is also a strong function of the clay mineral content as is shown in Figure 8.

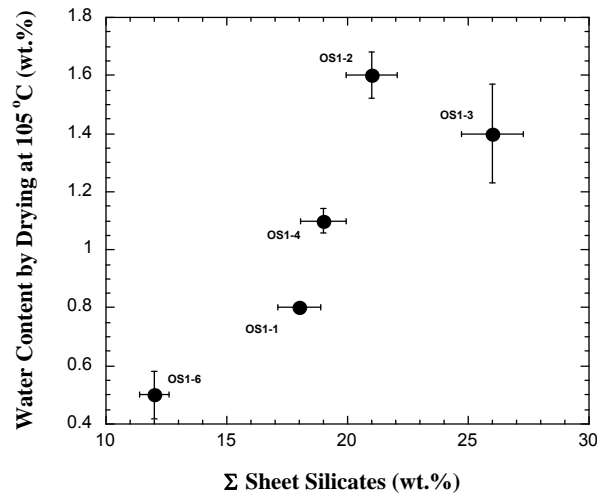


Figure 7 Gravimetric Water Content Obtained by Drying at 105°C as a Function of the Sum of Sheet Silicates, i.e., Clay Minerals (from Waber et al., 2007)

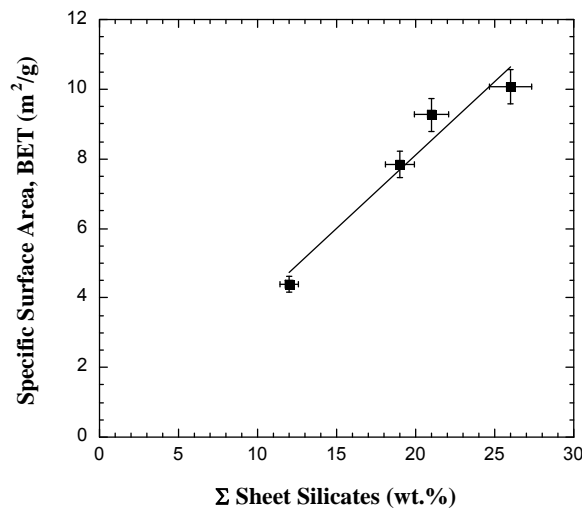


Figure 8 Specific Surface Area Versus Percentage of Clay Minerals (from Waber et al., 2007)

4.4 Diffusion Measurements

Measurements of molecular diffusion in core samples OS1-044.57 and OS1-075.97 from St. Mary's quarry have been conducted by the University of New Brunswick (UNB) (Al et al., 2007a; 2007b; 2007c). Figure 9 shows the photographs of the two core samples as received by UNB. The breaks in OS1-044.57 appear to be due to the higher content of clay minerals (dark layers) which caused planes of weakness where the core was easily broken during drilling operations. The grain density for each core was 2.7 g/cm³; the estimated total porosity was on average 4.4% for OS1-044.57 and 1.6% for OS1-075.97 (see Table 11). Al et al. (2007a) note that the higher porosity value may be biased by separation along the clay layers caused by stress relaxation and therefore may be unreliable.



Figure 9 Saturated Core Samples from Borehole OS1, St. Mary's Cement Quarry, Bowmanville

Table 11 Porosity and Grain Density Measurements for Samples from OS1

Sample	Grain density g/cm ³	Water-loss porosity %		Diffusion-accessible porosity %	
	Mean ± s.d. (n =4)	Range	Mean ± s.d. (n =4)	KI	HTO
OS1-044	2.73 ± 0.005	4.15 – 5.28	4.45 ± 0.55	3.2	4.7
OS1-075	2.72 ± 0.006	1.30 – 1.98	1.65 ± 0.28	0.7	1.2

Sample OS1-044.57 was tested with a potassium iodide (KI) tracer in a through-diffusion cell to determine the effective diffusion coefficient (D_e) for iodide normal to the bedding plane. Figure 10 shows the linear diffusion profile for cumulative steady-state diffusion of 1 mol/L iodide yielding a value of $D_e = 1.24E-12$ m²/s and a diffusion-accessible porosity of 3.2%. The average water-loss porosity for this sample was estimated gravimetrically as 4.4% and the diffusion-accessible porosity between 3.2% and 4.7% depending on tracer (see Table 11). Table 12 presents the results for through-diffusion using iodide and tritium (HTO) tracers. The results are higher for tritium than iodide; a similar result was reported by Van Loon et al. (2003).

A pore-water diffusion coefficient (D_p) is determined by the X-ray radiography diffusion technique, whereas in conventional through-diffusion type experiments, an effective diffusion coefficient (D_e) is determined. The apparent diffusion coefficient can be related to the effective diffusion coefficient by (Van Loon et al. 2004):

$$D_e = \alpha D_p = (\varepsilon + \rho \cdot K_d) D_p$$

where α is the rock capacity factor; ε is the diffusion accessible porosity; ρ = the bulk dry density and K_d is the distribution coefficient, which = 0 for non-sorbing solutes such as iodide, therefore $\alpha = \varepsilon$, when $K_d = 0$.

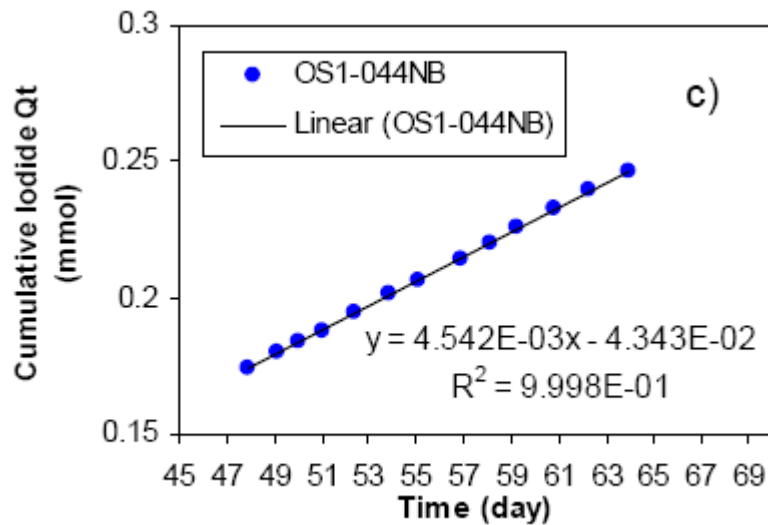


Figure 10 Determination of D_e and α for Clay-rich Core from St. Mary's Quarry

Table 12 Summary of Diffusion Properties of Surrogate Cores by the Through-Diffusion Method

	Source reservoir	Diffusion properties	OS1-044NB	OS1-075NB
KI tracer	1 M	D_e (m^2/s)	1.2×10^{-12}	2.1×10^{-13}
		Rock capacity factor α (%)	3.2	0.7
	0.1 M	D_e (m^2/s)	1.6×10^{-12}	--
		Rock capacity factor α (%)	3.1	--
HTO tracer	40,000-50,000 Bq/mL	D_e (m^2/s)	4.0×10^{-12}	2.6×10^{-13}
		Rock capacity factor α (%)	4.7	1.2
	5,000 Bq/mL	D_e (m^2/s)	3.0×10^{-12}	--
		Rock capacity factor α (%)	4.9	--

Effective diffusion coefficients from x-ray radiography presented in Table 13 identify the diffusion direction with respect to bedding planes, i.e., 'NB' indicates that the measurement was conducted normal to bedding planes and 'PB' refers to tests conducted parallel to bedding. The estimates of D_e by the two methods are notable for

the similarity in estimates for OS1-044NB and OS1-075NB, given the very different means of measurement between the through-diffusion method of Figure 10 and the X-ray radiography of Figure 11. Importantly, the difference in the diffusion estimates between the two core samples is explained by Boving and Grathwohl's (2001) observation that D_e is a function of the porosity. Local heterogeneities rather than anisotropy in diffusion appear to explain the differences between the cores measured normal to bedding planes and those measured parallel to bedding planes suggesting that pore networks are continuous in both directions. A complete list of diffusion properties from X-ray radiographic testing is presented in Appendix C.

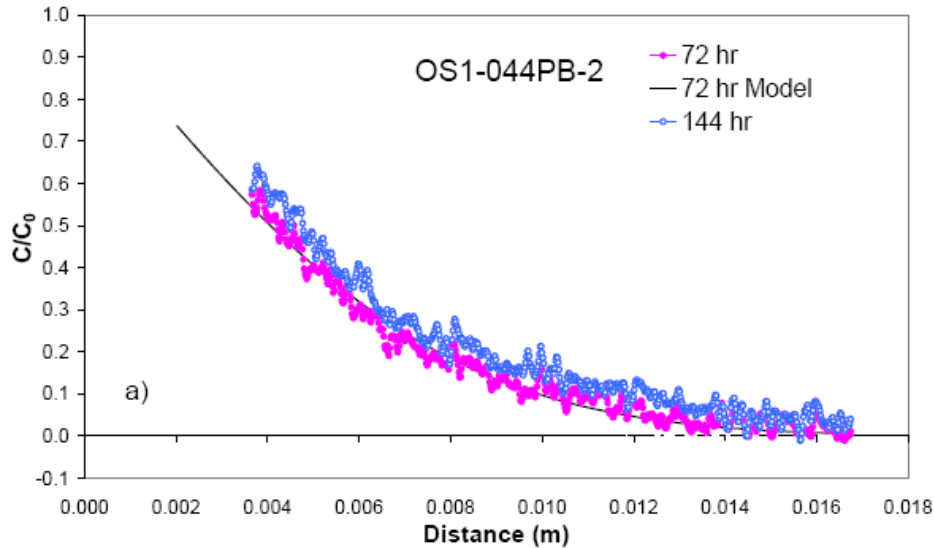


Figure 11 Diffusion Profile by X-ray Radiography on Sample OS1-044, Parallel to Bedding

Table 13 Summary of Diffusion Properties for Surrogate Cores by X-Ray Radiography and Through-Diffusion using 1 mol/L KI Tracer

Sample ID	X-ray Radiography		Through-diffusion	
	D_p (m^2/s)	$D_e = D_p \cdot \alpha$ (m^2/s)	D_e (m^2/s)	α (%)
OS1_044NB	4.5×10^{-11}	1.4×10^{-12}	1.2×10^{-12}	3.2
OS1_044PB	4.8×10^{-11}	3.5×10^{-13}	-	-
OS1_075NB	4.8×10^{-11}	3.5×10^{-13}	2.1×10^{-13}	0.7
OS1_075PB	6.3×10^{-11}	4.6×10^{-13}	-	-

4.5 Porewater Extraction

Core samples for porewater extraction were sent to three different laboratories; each to test a different technique to extract porewater samples and analyze for geochemical parameters: (1) the US Geological Survey for ultracentrifugation (Gascoyne et al., 2007), (2) the University of Bern for crush & leach, out diffusion, diffusive equilibration and advective displacement (Waber et al., 2007), and (3) the University of Ottawa for crush & leach and vacuum distillation. The ultracentrifugation tests were not conducted as part of the DGR study and therefore are not presented here.

4.5.1 UniBern

A more direct and traditional method for determining porewater composition is by crushing the core and then leaching it with distilled, deionized water, i.e., ‘crush & leach’. The criterion for acceptable crush and leach results is that the aqueous extracts plot in linear pattern for all ratios of solids (i.e., crushed rock particles) to liquids (i.e., porewater extracts). This S:L ratio may also permit the identification of unwanted effects of the crush and leach operation, such as the dissolution and oxidation of sulphide minerals causing elevated sulphate concentrations and calcite dissolution. Figures 12 and 13 shows the S:L ratios for anions and cations respectively. Each sample shown these figures was prepared and analysed in duplicate and error bars indicate errors of $\pm 5\%$. Waber et al. (2007) found that the differences in Ca^{2+} concentrations and total alkalinity in the extract solutions of samples OS1-1 and OS1-6 and samples OS1-2 and OS1-3 were “related to the differences in the mineralogical composition of these samples and the grain size used in the extraction test. Sample OS1-6 (and most probably also OS1-1) has more than twice the amount of pyrite/marcasite than samples OS1-2 and OSI-3.” Because the S:L ratio in-situ for a rock with brine-filled porosity of 3% ($S_B = 100\%$) is ~ 80 , extrapolation of linear parameter ratios provides an estimate of the actual pore-water composition. Thus, chloride produced at a S:L = 1 was ~ 2.2 g/L that would indicate a pore-water chloride ion concentration ~ 180 g/L at an S:L = 80.

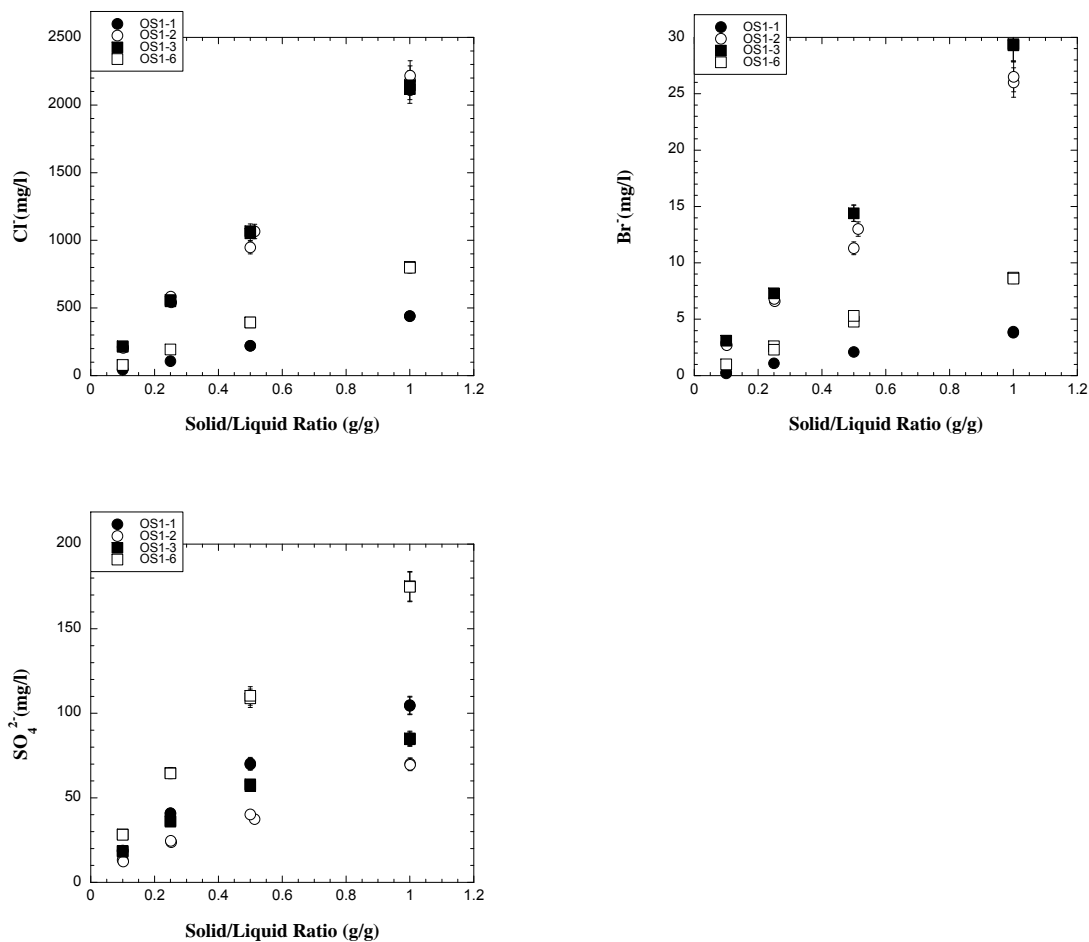


Figure 12 Anion Concentrations in Aqueous Extract Solutions of Cobourg Limestone Samples as a Function of Solid:Liquid Ratios.

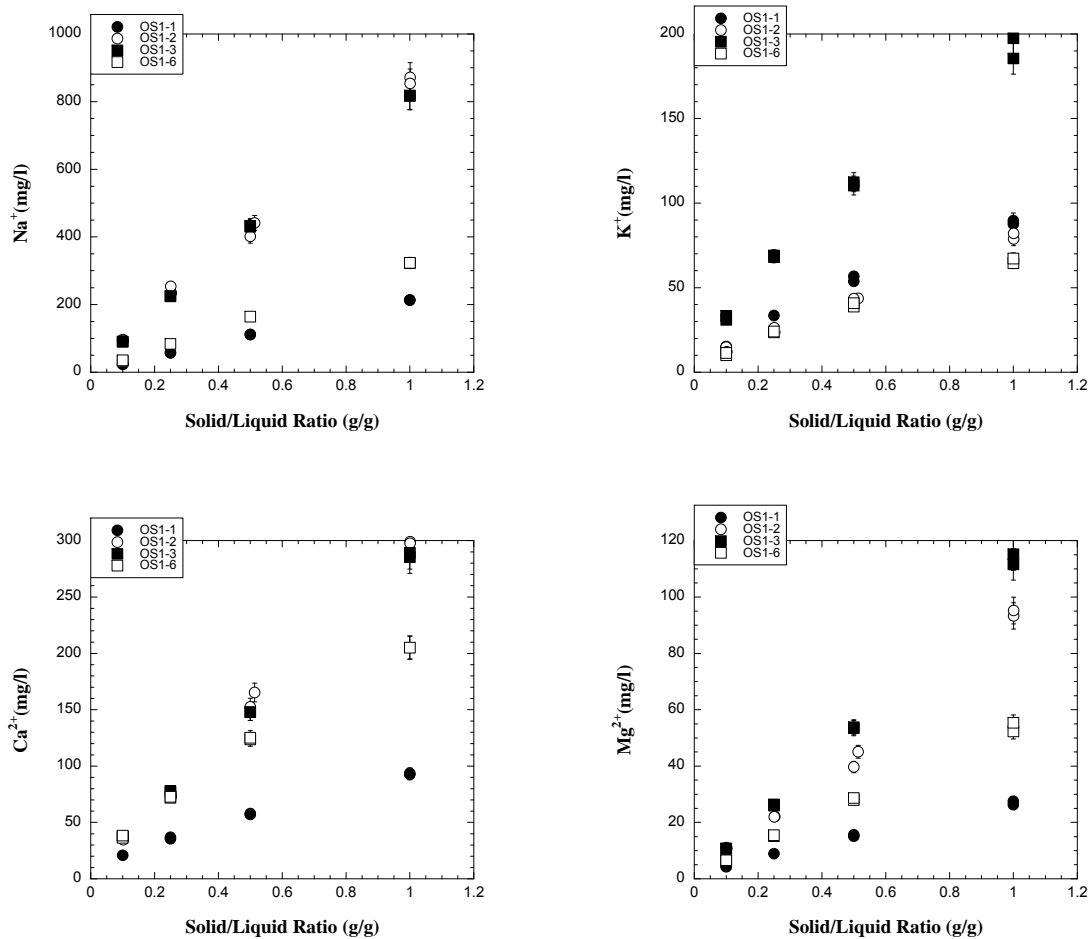


Figure 13 Cation Concentrations in Aqueous Extract Solutions of Cobourg Limestone Samples as a Function of Solid:Liquid Ratios.

Waber et al. (2007) also found that the nickel ethylenediamine solution used in cation exchange studies was useful in estimating the cation exchange capacity of the clay-sized fraction of the core provided the clay mineral sorbents were quantified. Thus the Ni²⁺ ion sorbed strongly to the clay sites and de-sorbed the resident cations. However, it is not possible to use this method to determine this exchangeable cation population because the extreme salinity of the porewaters interferes with the detection of the relatively small quantity of the exchangeable ions.

Out-diffusion experiments have been used to measure the pore-water chemistry of granitic rocks and provide a means by which the conservative ions – those not susceptible to mineral or redox reactions during the experiment – might be estimated. Waber et al (2007) measured an equilibrium diffusion profile for both the chloride and bromide ions after approximately 50 days. The results – probably the most reliable pore-water data presently available – are presented in Table 14. Table 14 shows the best estimate and the plus (+) and minus (-) errors associated with chloride and bromide concentrations in Cobourg Formations cores from Bowmanville.

Table 14 Apparent Concentrations of Chloride and Bromide Ions in Pore Water from OS1-56.49

Sample	Cl g/kg _{H2O}	Cl +error g/kg _{H2O}	Cl -error g/kg _{H2O}	Br g/kg _{H2O}	Br +error g/kg _{H2O}	Br -error g/kg _{H2O}
OS1-4	128.3	13.6	11.1	1.65	0.18	0.14

While crush and leach, out diffusion and ultracentrifugation provide means of varying reliability by which the concentration of aqueous ions may be measured, other techniques are required for the measurement of environmental isotopes such as ¹⁸O and ²H (deuterium). Isotope diffusive exchange and advective displacement have been investigated at the University of Bern. It appears possible to obtain pore-water samples by diffusive equilibration if the salinity of the pore water is similar to that of the test water into which the isotopes diffuse; that is, a certain amount of successful 'guesswork' is required a priori to obtain a test sample suitable for mass spectrometry. The mass spectrometry also presents difficulty because the problems arising from analysis of saline solutions. Samples from UniBern are to be analyzed at the University of Lausanne in Switzerland and at the University of Ottawa after which time it will be better understood what further development is required or if other approaches to pore-water extraction are more promising.

Advective displacement of pore water was developed at UniBern by Mader (2004) for extraction of the Opalinus Clay. It involves the use of a high hydraulic gradient (~ 5 MPa) across a core segment of 76 mm diameter by 56 mm length and the injection of artificial pore water (APW) to displace the pore water contained within the core. Results from OS1-62.43 are presented in Table 15. F.J. Pearson expressed concern that the high imposed hydraulic gradients might cause mineral precipitation and/or dissolution. Mader (in Waber, 2007) indicated that the reduction in volume of fluid produced from the 1st aliquot (1.2 g) to the 2nd (0.97 g) to the 3rd (0.85 g) was due to pore plugging, perhaps due to mineral precipitation.

Table 15 Composition of Extracted Pore-Water Aliquots and the Artificial Pore Water (APW), where APW (d) was the Design Na-Cl-Ca-SO₄ Pore Water and OS1-5 indicates Core Sample OS1-62.43

	OS1-5-1st		OS1-5-2nd		OS1-5-3rd		APW analyzed		APW (d)
	g/l	mol/l	g/l	mol/l	g/l	mol/l	g/l	mol/l	mol/l
Na	53.76	2.338	58.83	2.559	64.73	2.816	105.32	4.581	6.128
K	0.68	0.017	0.73	0.019	0.77	0.020	np	np	np
Mg	6.74	0.277	5.75	0.237	3.86	0.159	np	np	np
Ca	16.11	0.402	12.78	0.319	10.55	0.263	0.077	0.0019	0.0082
Sr	0.46	0.0053	0.46	0.0053	0.40	0.0046	np	np	np
F	0.01	0.0005	<0.005	<0.0002	<0.005	<0.0002	np	np	np
Cl	117.0	3.301	131.1	3.698	131.5	3.708	139.4	3.932	5.119
Br	1.12	0.014	1.01	0.013	0.83	0.010	np	np	np
SO ₄	0.78	0.008	1.02	0.011	1.21	0.013	31.45	0.327	0.442
NO ₃	1.46	0.024	2.36	0.038	3.03	0.049	6.74	0.109	0.142
Balance %		5.2		0.9		1.4		1.2	0
NO ₃ /APW	0.22		0.35		0.45				
Br (in-situ)	1.43	0.018	1.55	0.019	1.51	0.019			
Cl (in-situ)	110.9	3.127	126.7	3.572	125.0	3.525			

4.5.2 University of Ottawa

Crush and leach estimates of porewater chemistry were obtained by the University of Ottawa (Clark and Mohapatra, 2007) following vacuum extraction of the cores (S:L~0.9). Table 16 shows the concentrations of anions; the very high concentrations of sulphates when compared with the data of Waber et al. (< 200 mg/L at all S:L <1) suggests that pyrite oxidation may be responsible. However, pore-water chloride concentrations, ranging from 104 g/kg to 228 g/kg, are similar to those measured by UniBern by out-diffusion (i.e., 128 g/kg). In terms of molal ratios, the University of Ottawa data is similar to that of the University of Bern with mBr/mCl-varying between 5.2 to 6.5E-03; UniBern data ranges from 3.8 to 6.4E-03. Halite was not detected by SEM/EDS, x-ray diffraction nor by optical petrography, therefore the Br/Cl ion ratios appear to be representative.

Table 16 Crush and Leach Concentrations (Clark and Mohapatra, 2007)

Sample No.	Cl ⁻ (ppm)	Br ⁻ (ppm)	SO ₄ ²⁻ (ppm)
OS1-071.02-L3	228,000	3,020	16,200
OS1-071.02-L8	104,000	1,460	7,710
OS1-051.28-L11	120,000	1,640	5,850
OS1-051.28	179,000	2,600	9,780
OS1-051.28*	166,000	1,960	9,840

Stable oxygen and hydrogen isotopes were measured following vacuum distillation at 150°C as recommended by Altinier et al. (2006). Figure 14 indicates that the samples fell close to the Global Meteoric Water Line (GMWL) where it is intersected by the axis of samples measured in the Michigan Basin. The reliability of these results awaits comparison with other methods of pore-water extraction and analysis and further analytical testing.

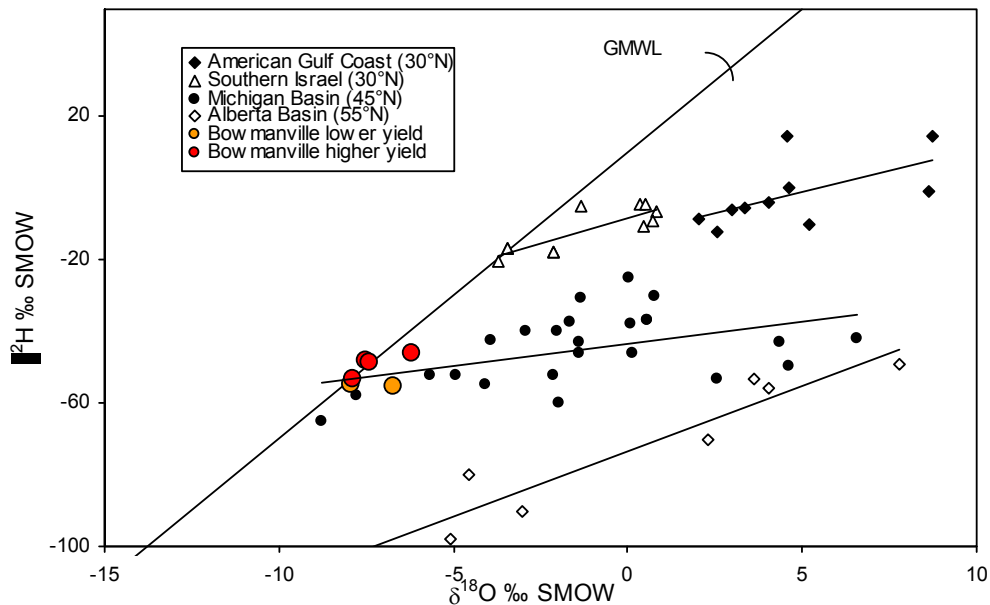


Figure 14 Stable Isotopes of Oxygen and Hydrogen for the Bowmanville Cores

5 Data Quality and Use

Data presented in this report represent an initial evaluation of core testing procedures and laboratories for use in the Bruce DGR site characterization program. While the initial results indicate favourable and less favourable directions for laboratory core testing procedures, final decisions on the suitability of the specific core testing methods evaluated in this TR to the Bruce DGR program, should await initial test results on DGR core obtained in 2007, and the results of other core testing programs undertaken through the Nuclear Waste Management Organization's Technology Research and Development Program.

Data on the geological, petrophysical, diffusion and porewater properties of Cobourg Formation core collected from Bowmanville are representative of shallow disturbed bedrock remote from the Bruce DGR site and should not be used to infer core properties from the Bruce DGR site.

6 Conclusions

The preserved surrogate core samples of Cobourg Formation argillaceous limestone recovered at St. Mary's quarry were distributed to seven laboratories for mineralogical, petrographic, geochemical, petrophysical and isotopic characterization. The St. Mary's quarry core is a fossiliferous limestone with a mud matrix, i.e., a wackestone. Diffusion measurements by through-diffusion and x-ray radiography appear to work well with Cobourg cores and, by virtue of their low porosity, are likely to be readily measured on other Paleozoic limestones and shales at the DGR. The cores exhibit low permeability ($k_v \sim 1\text{E-}20 \text{ m}^2$) and low total porosity (~1-5%) with an effective iodide diffusion coefficient of the order of $\sim 1\text{E-}12 \text{ m}^2/\text{s}$ at 3% porosity and $\sim 1\text{E-}13 \text{ m}^2/\text{s}$ at 1% porosity.

Petrophysical testing of Bowmanville cores for permeability has focussed on gas pulse permeability tests. Future testing programs should consider hydraulic pulse permeability tests to mitigate the complications of multi-phase (gas-brine) flows and gas slippage/compression often associated with gas pulse permeability testing.

It is not yet clear whether diffusive equilibration and advective displacement provide reliable methods for porewater extraction. Further development is being undertaken of advective displacement with DGR-2 cores and test samples extracted by diffusive equilibration are to be analysed at the Universities of Ottawa and Lausanne.

However, the following techniques provide preliminary estimates for the porewater characterization of the deep geological repository proposed for the Bruce site:

- a) Standard methods of crush & leach for major ions, provided that provision is made to prevent sulphide mineral oxidation in the case of sulphate;
- b) Vacuum distillation at 150°C to recover stable oxygen and hydrogen isotopes; and
- c) Out diffusion for chloride and bromide.

7 References

Actlabs, 2006a. Petrographic Study of a Fossiliferous Limestone. Report prepared by E. Schandl, Geoconsult, Toronto for Activation Laboratories, Ancaster, Ontario, November 10.

Actlabs, 2006b. Report A06-3972, 4 p., Ancaster, Ontario.

Al, T., Y. Xiang, and L. Cavé, 2007a. Measurement of Diffusion Properties by X-ray Radiography: Surrogate

Core Samples from St. Mary's Cement Quarry, Bowmanville, Ontario. Progress Report 1: 12 February, 2007, Dept. of Geology, University of New Brunswick, Fredericton, NB, 7 p.

Al, T., Y. Xiang, and L.Cavé, 2007b. Measurement of diffusion properties by X-ray radiography and by through-diffusion techniques using KCl tracer: Surrogate core samples from St. Mary's Cement Quarry, Bowmanville, Ontario. Progress Report 2. 4 May, 2007, Dept. of Geology, University of New Brunswick, Fredericton, NB, 9 p.

Al, T., Y. Xiang, and L.Cavé, 2007c. Measurement of diffusion properties by X-ray radiography and by through-diffusion techniques using KCl tracer: Core samples from OS1 and DGR2. Progress Report 3. 11 October, 2007, Dept. of Geology, University of New Brunswick, Fredericton, NB, 9 p.

Altinier, M.V., S. Savoye, J.-L. Michelot, C. Beaucaire, M. Massault, D. Tessier and H.N. Waber, 2006. The isotopic composition of pore-water from Tournemire argillite (France) : An inter-comparison study. *J. Physics & Chemistry of the Earth*, doi:10.1016/j.pce.2006.02.047.

Boving, T.B. and P. Grathwohl, 2001. Tracer diffusion coefficients in sedimentary rocks: correlation to porosity and hydraulic conductivity. *Journal of Contaminant Hydrology* 53:85-100.

Clark, I.D. and R. Mohapatra, 2007. Bowmanville and DGR-1 Surrogate Core Analysis: Methods for Analysis of Pore Water, Isotopes, Geochemistry and He. Dept. of Earth Sciences, Faculty of Science, University of Ottawa, 35 p.

Gabrielyan, K., 2006. X-ray diffraction and scanning electron microscopic analysis of the limestone sample. December 21, 2006, Actlabs, Ancaster, ON.

Gascoyne, M., Z.E. Peterman, K. Scofield and M. Hobbs, 2007. Matrix pore waters – ultracentrifugation method for sedimentary rocks. March 27th, 2007.

Intera Engineering Ltd., 2007a. Project Quality Plan, DGR Site Characterization, Revision 3, January 17, Ottawa.

Intera Engineering Ltd., 2007b. Test Plan for Laboratory Petrophysical Testing of DGR-2 Core, TP-07-03, Revision 1, May 28.

Intera Engineering Ltd., 2006a. Geoscientific Site Characterization Plan, OPG's Deep Geologic Repository for Low and Intermediate Level Waste, Report INTERA 05-220-1, OPG 00216-REP-03902-00002-R00, April, Ottawa.

Intera Engineering Ltd., 2006b. Test Plan for Off-Site Drill Core Collection and Preservation, TP-06-01, Revision 0, August 28, Ottawa.

Jones, F.O. and W.W. Owens, 1979. A laboratory study of low permeability gas sands. *SPE* 7551, 10p.

Jones, S.C., 1997, A technique for faster pulse-decay permeability measurements in tight rocks, *SPE Formation Evaluation* 12(1): 19-26.

Mäder, U.K., Waber, H.N., Gautschi, A., 2004. New method for pore water extraction from claystone and determination of transport properties with results for Opalinus Clay (Switzerland). In: R.B. Wanty, R.R. Seal II (Eds.), *Water-Rock Interaction: Proc. 11th Internat. Symp. on Water-Rock Interaction - WRI-11*, Saratoga Springs, NY, USA, A. A. Balkema, The Netherlands, p. 445-449.

Stumm, W., 1992. *Chemistry of the Solid-Water Interface*. Wiley-Interscience, New York.

Swanson, B.F., 1981. A simple correlation between permeabilities and mercury capillary pressures. *Journal of Petroleum Technology*, pp. 2498-2504.

Van Loon, L., J.M. Soler, and M.H. Bradbury, 2003. Diffusion of HTO, $^{36}\text{Cl}^-$ and $^{125}\text{I}^-$ in Opalinus Clay samples from Mont Terri: Effect of Confining Pressure. *Journal of Contaminant Hydrology* 61:73-83.

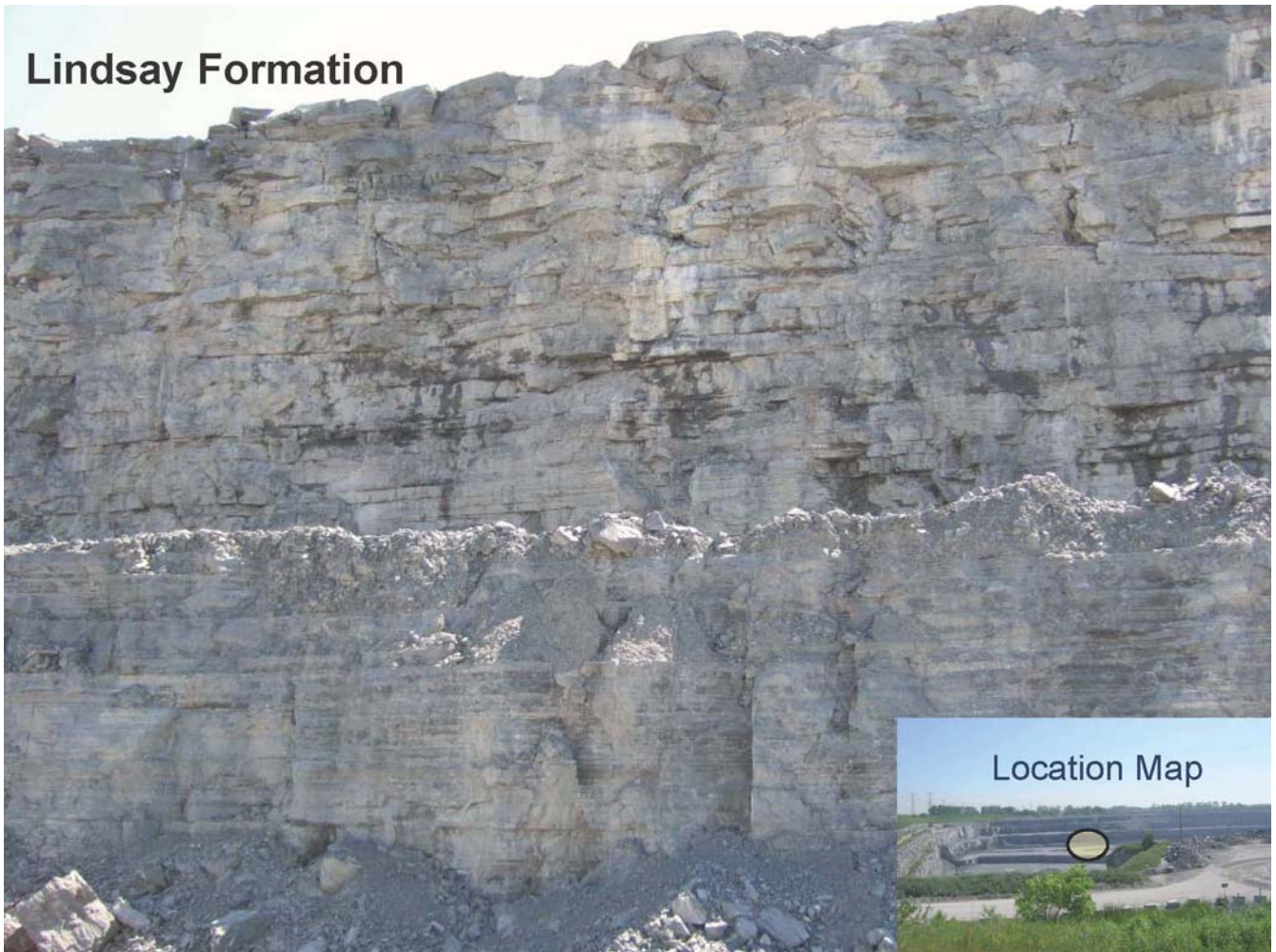
Van Loon, L., J.M. Soler, W. Muller, and M.H. Bradbury, 2004. Anisotropic diffusion in layered argillaceous rocks: A case study with Opalinus Clay. *Environmental Science & Technology* 38:5721-5728.

Waber, H.N., 2007. Testing Methods for the Characterization of Saline Pore Water in an Ordovician Limestone (Cobourg formation, St. Mary's Quarry, Ontario): Feasibility Study. Institute of Geological Sciences, University of Bern, Switzerland, Technical Report TR 07-01, August 2007.

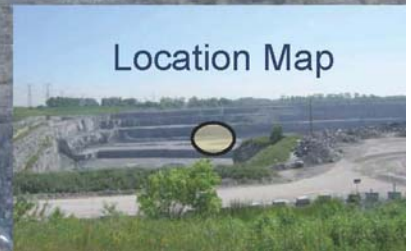
APPENDIX A

Photograph of the Cobourg (Lindsay) Formation at St. Mary's Quarry (by Derek Martin, University of Alberta)

Lindsay Formation



Location Map



APPENDIX B

Photographs of Cores

APPENDIX C

Diffusion Properties for Surrogate Cores by X-ray Radiography

Sample ID	Time (h)	D_p (m^2/s) measured	Water-loss porosity (%)	Fitted porosity (%) ϕ_{fit}	D_e (m^2/s) = $D_p \cdot \phi_{fit}$	Diffusion-accessible porosity (%) α	D_e (m^2/s) = $D_p \cdot \alpha$							
OS1-044NB	89	7.5×10^{-11}	4.5 ± 0.6	5.5	4.1×10^{-12}	3.2	2.4×10^{-12}							
	161	4.5×10^{-11}			2.5×10^{-12}		1.4×10^{-12}							
OS1-044PB	89	5.0×10^{-11}		4.5	4.5		2.5×10^{-12}	3.2	1.6×10^{-12}					
	161	4.5×10^{-11}					2.3×10^{-12}		1.4×10^{-12}					
OS1-044PB2	72	5.0×10^{-11}		4.0	4.0		2.0×10^{-12}		3.2	1.6×10^{-12}				
	144	3.0×10^{-11}					1.2×10^{-12}			9.5×10^{-13}				
OS1-075NB	89	6.4×10^{-11}		1.7 ± 0.3	3.0		1.9×10^{-12}			0.7	4.7×10^{-13}			
	161	6.0×10^{-11}					1.8×10^{-12}				4.4×10^{-13}			
OS1-075NB2	72	4.0×10^{-11}			4.5		4.5				1.4×10^{-12}	0.7	3.0×10^{-13}	
	144	3.5×10^{-11}									1.2×10^{-12}		2.6×10^{-13}	
OS1-075PB2	72	9.0×10^{-11}			3.6		3.6				3.2×10^{-12}		0.7	6.7×10^{-13}
	144	6.0×10^{-11}									2.2×10^{-12}			4.4×10^{-13}
OS1-075PB3	72	8.0×10^{-11}	4.8		4.8	3.8×10^{-12}	0.7				5.9×10^{-13}			
	144	6.5×10^{-11}				3.1×10^{-12}					4.8×10^{-13}			